RSC Advances

PAPER

View Article Online
View Journal | View Issue

Cite this: *RSC Adv.*, 2015, **5**, 31189

A new ICT and CHEF based visible light excitable fluorescent probe easily detects *in vivo* Zn^{2+}†

Krishnendu Aich,[a] Shyamaprosad Goswami,*[a] Sangita Das[a] and Chitrangada Das Mukhopadhyay[b]

Received 23rd February 2015
Accepted 23rd March 2015

DOI: 10.1039/c5ra03353e

www.rsc.org/advances

A new chelator and ICT donor based visible light excitable Zn^{2+} sensor was designed and developed by integrating quinoline and 2-hydroxy-3-(hydroxymethyl)-5-methylbenzaldehyde. The probe is sensitive towards Zn^{2+} in absorbance as well as in fluorescence experiments in 90% aqueous medium. The sensor demonstrates Zn^{2+}-specific emission enhancement due to the ICT and CHEF process with the LOD in the range of 10^{-8} M. The fluorescence quantum yield of the chemosensor is only 0.02, and it increases almost 11-fold (0.22) after complexation with Zn^{2+}. Interestingly, the introduction of other metal ions causes the fluorescence intensity to remain almost unchanged. Moreover, the ability of the probe (BQ) to sense Zn^{2+} in living cells has been explored.

Introduction

Detection and imaging of biologically relevant target molecules through fluorescence in living systems has emerged as an area of intense interest in the chemistry–biology interface owing to its significant biomedical implications.[1] Zn^{2+} has received considerable attention as it is the second most abundant heavy metal ion after iron present in the human body with a total content of 2–3 g in the whole body and a concentration as high as 10 μM in serum.[2] It is an essential nutrient required for normal growth[3] and development. It also plays crucial role for the key cellular processes such as DNA repair[4] and apoptosis.[5] A deficiency of zinc causes an imbalanced metabolism, which in turn can induce retarded growth in children, brain disorders, high blood cholesterol[6] and can also be implicated in various neurodegenerative disorders such as Alzheimer's disease, epilepsy, ischemic stroke, and infantile diarrhea.[7] Fluorescent Zn^{2+} imaging with Zn^{2+} sensors has demonstrated great success in providing temporal-spatial information of Zn^{2+} homeostasis in live cells.[8] Therefore, nowadays there is a huge demand for the development of Zn^{2+} chemosensors. Fluorescence spectroscopy is a powerful method for sensing and imaging metal cations at submicromolar concentrations.[9] In recent times, a number of selective and sensitive imaging tools capable of rapidly monitoring Zn^{2+} ions have been developed.[10] Specially development of sensitive sensors which can distinguish the metal ions with almost similar characteristic (like Zn^{2+}/Cd^{2+}, Pb^{2+}/Hg^{2+} pairs which may interfere in each other detection) are in high demand.

In the context of the above objectives and in continuation of our work,[11] in here, we have synthesized a highly sensitive and selective hydroxyquinoline based new visual and fluorescent probe BQ for Zn^{2+}. We have screened its potential applications in cell imaging and studied its cytotoxic properties. Interestingly here, Cd^{2+} is found to perturb the fluorescence a slight but the output is different from Zn^{2+}.

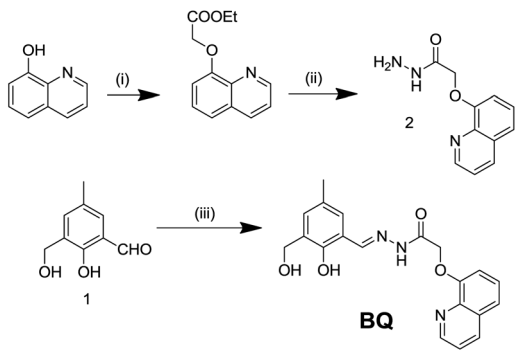

Scheme 1 Reagents and conditions: (i) ethylchloroacetate, K_2CO_3, dry acetone, reflux, 12 h. (ii) NH_2–NH_2, EtOH, reflux, 2 h, (iii) 2, EtOH, reflux, 6 h.

Results and discussion

Synthesis of BQ is accomplished by reaction of the compounds **2** and **1** in ethanol under refluxing condition for 6 h (Scheme 1). Compounds **1** and **2** were prepared from according to previously reported procedure.[12] The yield of the final imine functionalized

[a]*Department of Chemistry, Indian Institute of Engineering Science and Technology, Shibpur, Howrah-711 103, India. E-mail: spgoswamical@yahoo.com*

[b]*Centre for Healthcare Science & Technology, Indian Institute of Engineering Science and Technology, Shibpur, Howrah-711 103, India*

† Electronic supplementary information (ESI) available. See DOI: 10.1039/c5ra03353e

compound obtained to be 65%. The probe (BQ) was characterized by NMR and HRMS studies (Fig. S9–S11, ESI†).

Sensing studies

In order to investigate the metal-binding behavior of the probe (BQ) towards different cations, we have monitored both the UV-visible absorption and fluorescence study of BQ with different cations (Na^+, K^+, Mg^{2+}, Cu^{2+}, Mn^{2+}, Fe^{2+}, Fe^{3+}, Co^{2+}, Ni^{2+}, Cd^{2+}, Ca^{2+}, Zn^{2+} and Hg^{2+} as their chloride salts). All of the titration studies of BQ were carried out in CH_3OH–H_2O (1/9, v/v, 1 mM HEPES buffer at pH = 7.4) solution. The electronic absorption spectral behavior of BQ (10 μM) exhibited two sharp bands at 360 and 282 nm (Fig. 1a). Upon gradual addition of aqueous solution of Zn^{2+} (0–1.5 equiv.), the bands at 360 and 282 nm gradually decreased along with a new peak appeared at 405 nm, which readily increased with Zn^{2+} concentration. This new peak is being attributed to internal charge transfer (ICT) of BQ after interaction with Zn^{2+}. This spectral behavior consecutively showed three well-defined isosbestic points centred at 380 nm, 340 nm and 305 nm.

Furthermore, BQ exhibits a good linear relationship of absorbance ratio (A_{405}/A_{282}) with added Zn^{2+} concentration (0 to 9 μM, Fig. S2, ESI†). The strong binding of Zn^{2+} with BQ was further supported by the association constant determined from Benesi–Hildebrand plot[13] by using UV-vis data and it was found to be 5.77×10^5 M^{-1} (Fig. S4, ESI†). Notably, the addition of other metal cations did not perturb the initial absorption spectrum of the chemosensor significantly (except Cu^{2+}, in here a slight change was noticed). From these UV-vis spectral studies, it is obvious that the probe BQ revealed a very high affinity towards Zn^{2+} in the ground state.

The fluorescence spectrum of the probe BQ (10 μM) exhibited a weak emission band centered at 435 nm in CH_3OH–H_2O solution (1/9, v/v, 1 mM HEPES buffer at pH = 7.4) upon excitation at 400 nm. On incremental addition of Zn^{2+} (0–1.5 equiv.) to the solution of the probe BQ, the fluorescence emission exhibited an enhancement along with a red shift from 435 nm to 475 nm. This dramatic red shift (~40 nm) of the fluorescence of BQ after introduction of Zn^{2+} was attributed to the internal charge transfer (ICT). In addition, the emission band at 475 nm significantly enhanced after incremental addition of Zn^{2+} (Fig. 2a). During the course of titration the intensity at 475 nm

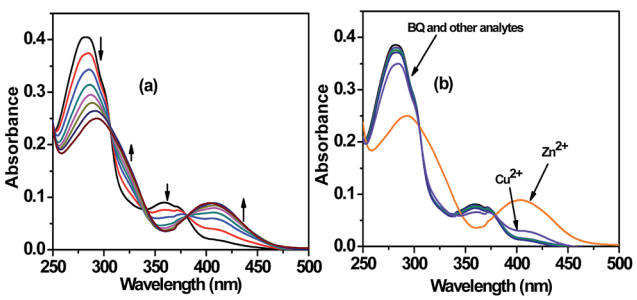

Fig. 1 UV-vis spectra of BQ (10 μM) in CH_3OH–H_2O solution (1/9, v/v, pH = 7.4) in presence of (a) Zn^{2+} (0–1.5 equivalents) and (b) different analytes (3 equivalents).

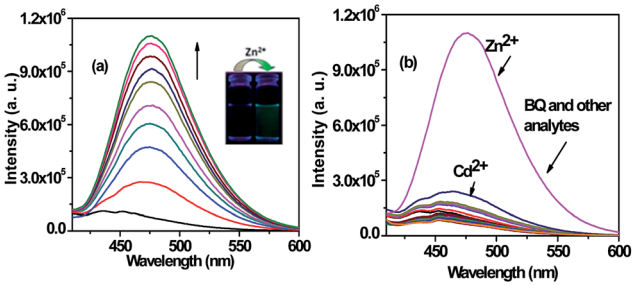

Fig. 2 Emission spectra of BQ (10 μM) in (MeOH–H_2O, 1/9, v/v, pH = 7.4) in presence of (a) Zn^{2+} (0–1.5 equivalents) and (b) different analytes (4 equivalents). Inset: emission colour change of BQ upon addition of 2 equivalents of Zn^{2+} after illumination under UV light. λ_{ex} = 400 nm.

(I_{475}) exhibited a beautiful linear relationship with Zn^{2+} concentration (0 to 9 μM, Fig. S1b, ESI†) with a R^2 value of 0.9807.

This overall spectral behavior of fluorescence enhancement of the probe BQ after being induced by Zn^{2+} may be due to the contribution of two mechanisms, namely ICT and CHEF mechanism. BPQ itself exhibited a weak fluorescence intensity at 435 nm, which may be due to the occurrence of *−E*, *−Z* isomerism for free rotation of the imine (–C=N) segment.

Now the introduction of Zn^{2+}, this kind of (*E*-, *Z*-) isomerism may stop and CHEF mechanism may came into play, which ultimately formed a stable chelate complex between the cation (Zn^{2+}) and the probe BQ. The addition of Zn^{2+} eventually made the system more rigid (Scheme 2) and revealed a fabulous increment in emission profile. The formation of 1 : 1 complexation with Zn^{2+} was confirmed by Job's plot (Fig. S6†) and HRMS data, it shows peaks at *m*/*z* 451.0923, which may be due to the formation of BQ–Zn^{2+} complex species.

Now selectivity and specificity are the two very important factors in order to evaluate the efficiency of any probe. So to prove the selectivity of the probe BQ toward Zn^{2+} ions, we carried out the fluorescence titration experiment of BQ in presence of other above mentioned cations. It was found that the probe was prone to Zn^{2+} only (selective enhancement of emission at 475 nm) and this affinity was very much prominent even in the presence of other guest metal ions (Fig. S7, ESI†). Thus all these experiments established that the probe BQ showed a major response only towards Zn^{2+} and it can detect exclusively Zn^{2+} at 475 nm without any noticeable interference. In the fluorescence titration experiment of BQ, a different

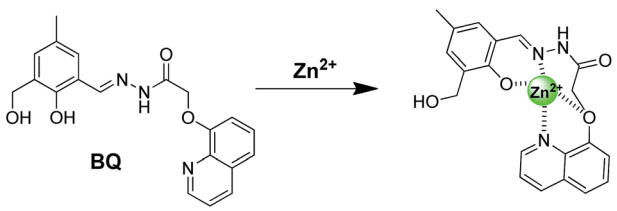

Scheme 2 Probable binding mode of BQ with Zn^{2+}.

interference was noticed with Cd^{2+}, it showed a slight change in emission at 465 nm but no interference at 475 nm. From this fluorescence experiment it was demonstrated that, the probe BQ was capable to detect back to back two of very similar cations with two different outputs (for Zn^{2+} it is a strong peak at 475 nm and for Cd^{2+} a weak peak at 465 nm). To determine the limit of detection *i.e.* how lower concentration of Zn^{2+} can be determined by the probe (BQ), we recorded the fluorescence data using 10 μM solution (CH_3OH–H_2O, 1/9, v/v, 1 mM HEPES buffer, pH = 7.4) of BQ (Fig. S1b, ESI†). The detection limit of BQ for Zn^{2+} was determined to be 2.35×10^{-8} M, using the equation $DL = K \times Sb_1/S$, where $K = 3$, Sb_1 is the standard deviation of the blank solution and S is the slope of the calibration curve[14] (Fig. S1, ESI†).

pH study

In order to examine the pH sensitivity of our probe BQ, we examined the acid–base titration experiment. From the titration study it was observed that BQ does not undergo any noticeable change in the fluorescence profile within the pH range from 2–8. But in strong basic conditions (pH > 9), deprotonation of the phenolic group causes the coloration along with strong green fluorescence (Fig. S8a, ESI†). Thus BQ can be employed for the detection of Zn^{2+} in near-neutral pH range (pH = 7.4). The pH sensitivity of BQ in presence of Zn^{2+} was also studied. The results revealed that in strong acidic pH (<3) and in strong basic pH (>10) detection of Zn^{2+} was a little bit hampered. But in the pH range of 3 to 9, BQ can detect Zn^{2+} with no such interference (Fig. S8b, ESI†).

Live-cell imaging study

Cell viability assay. Considerations of the practical application of thermodynamic favourable binding properties of BQ with Zn^{2+} led to the further examination of the ability of the probe (BQ) to sense Zn^{2+} in the living cells. In order to fulfil this objective it is important to determine the cytotoxic effect of BQ and Zn^{2+} and the complex on live cells. The well-established MTT assay, which is based on mitochondrial dehydrogenase activity of viable cells, was adopted to study cytotoxicity of above mentioned compounds at varying concentrations mentioned in method section. Fig. 3 shows that probe compound did not exert any adverse effect on cell viability; same is the case when cells were treated with varying concentrations of $ZnCl_2$. However, exposure of HCT cells to probe–Zn^{2+} complex resulted in a decline in cell viability above 20 μM concentration.

The effect was more pronounced in higher concentration and showed an adverse cytotoxic effect in a dose-dependent manner. The viability of HCT cells was not influenced by the solvent (DMSO) as evidenced in Fig. 3, leading to the conclusion that the observed cytotoxic effect could be attributed to probe–Zn^{2+} complex. The results obtained in the *in vitro* cytotoxic assay suggested that, in order to pursue fluorescence imaging studies of probe–Zn^{2+} complex in live cells, it would be prudent to choose a working concentration of 10 μM for probe compound.

Imaging of cells. Fluorescence microscopic studies revealed a lack of fluorescence for RAW cells when treated with either probe compound (10 μM) or $ZnCl_2$ (20 μM) alone (Fig. 4, panel a & b).

Upon incubation with $ZnCl_2$ followed by probe compound a striking green fluorescence was observed inside RAW cells, which indicated the formation of probe–Zn^{2+} complex, as observed earlier in solution studies. Further, an intense green fluorescence was conspicuous in the perinuclear region of RAW cells (Fig. 4, panel b) which indicates that the probe can penetrate cell membrane easily and can be used to detect Zn^{2+} in cells. The fluorescence microscopic analysis strongly suggested that probe could readily cross the membrane barrier, permeate

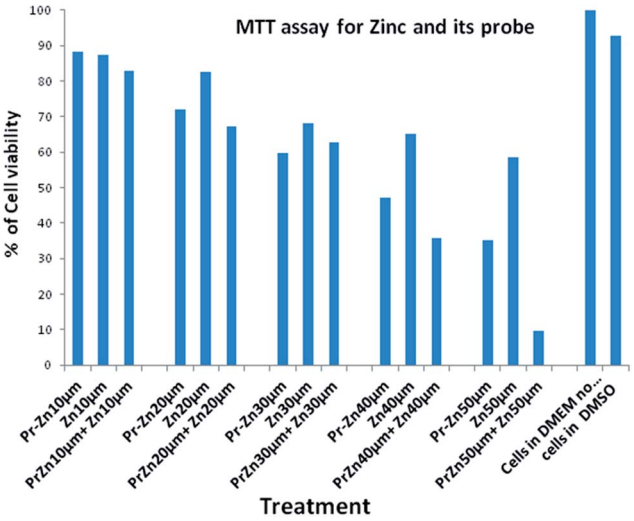

Fig. 3 It represents % cell viability of HCT cells treated with different concentrations (10 μM to 50 μM) of BQ for 12 h determined by MTT assay. Results are expressed as mean of three independent experiments.

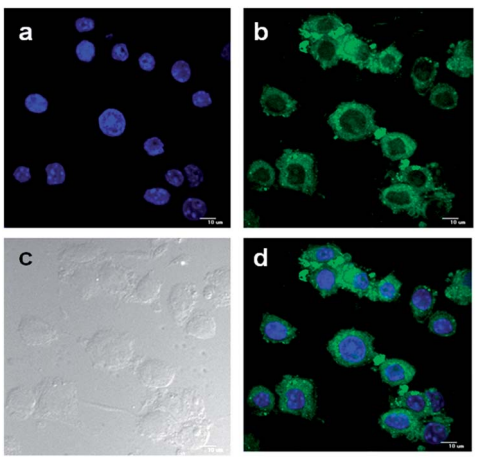

Fig. 4 Confocal microscopic images of probe in RAW 264.7 cells pretreated with $ZnCl_2$: (a) $ZnCl_2$ treatment only at 2.0×10^{-5} M concentration, nuclei counterstained with DAPI (1 μg mL^{-1}), (b) treatment a followed by probe BQ at concentration 1.0×10^{-5} M, (c) bright field image of the cells after treatment (d) overlay image in dark field. All images were acquired with a 60× objective lens with a scale bar of 10 μm. $\lambda_{ex} = 400$ nm.

into RAW cells, and rapidly sense intracellular Zn^{2+}. It is significant to mention here that bright field images of treated cells did not reveal any gross morphological changes, which suggested that RAW cells were viable. These findings open up the avenue for future *in vivo* biomedical applications of the probe to image intracellular Zn^{2+}.

Experimental

General

Unless otherwise mentioned, materials were obtained from commercial suppliers and were used without further purification. Thin layer chromatography (TLC) was carried out using Merck 60 F_{254} plates with a thickness of 0.25 mm. Melting points were determined on a hot-plate melting point apparatus in an open-mouth capillary and are uncorrected. ^1H and ^{13}C NMR spectra were recorded on JEOL 400 MHz and 125 MHz instruments respectively. For NMR spectra, $CDCl_3$ and d^6-DMSO were used as solvents using TMS as an internal standard. Chemical shifts are expressed in δ units and ^1H–^1H and ^1H–C coupling constants in Hz. UV-vis spectra were recorded on a JASCO V-630 spectrometer. Fluorescence spectra were recorded on a Perkin Elmer LS 55 fluorescence spectrometer. IR spectra were recorded on a JASCO FT/IR-460 plus spectrometer, using KBr discs. For the titration experiment, we use the cations *viz.* [Na^+, K^+, Mg^{2+}, Cu^{2+}, Mn^{2+}, Fe^{2+}, Fe^{3+}, Co^{2+}, Ni^{2+}, Ca^{2+}, Cd^{2+}, Zn^{2+} and Hg^{2+} as their chloride salts.

General method of UV-vis and fluorescence titration

UV-vis method. For UV-vis titrations, stock solution of the receptor (10 μM) was prepared in [(CH_3OH–water), 1/9, v/v] (at 25 °C) using 1 mM HEPES buffered pH 7.4 solution. The solutions of the guest cations using their chloride salts in the order of 1×10^{-5} M, were prepared in deionized water using HEPES buffer at pH = 7.4. Solutions of various concentrations containing the sensor and increasing concentrations of cations were prepared separately. The spectra of these solutions were recorded by means of UV-vis method.

Fluorescence method. For fluorescence titrations, stock solution of the sensor (10 μM) used was the same as that used for UV-vis titration. The solutions of the guest cations using their chloride salts in the order of 1×10^{-5} M, were prepared same as stated in UV-vis experiment. Solutions of various concentrations containing sensor and increasing concentrations of cations were prepared separately. The spectra of these solutions were recorded by means of fluorescence method.

Determination of fluorescence quantum yield. To determine the quantum yields of BQ and BQ–Zn^{2+}, we recorded their absorbance in methanol solution. The emission spectra were recorded using the maximal excitation wavelengths, and the integrated areas of the fluorescence-corrected spectra were measured. The quantum yields were then calculated by comparison with fluorescein ($\Phi_s = 0.97$ in basic ethanol) as reference using the following equation:

$$\Phi_x = \Phi_s \times (I_x/I_s) \times (A_s/A_x) \times (n_x/n_s)^2$$

where, x & s indicate the unknown and standard solutions respectively, Φ is the quantum yield, I is the integrated area under the fluorescence spectra, A is the absorbance and n is the refractive index of the solvent.

Synthetic method for the preparation of the probe. To the stirred solution of compound **2** (0.25 g, 1.15 mmol) in ethanol, 2-hydroxy-3-(hydroxymethyl)-5-methylbenzaldehyde (0.2 g, 1.20 mmol) was added and the reaction mixture was refluxed for 6 hours. After ensuring that the reactants were fully consumed, by checking TLC, the reaction mixture was allowed to cool to room temperature. A white precipitate appeared which was filtered, washed with cold ethanol (1 mL × 2) and dried in air. Yield = (0.27 g) 65%.

^1H NMR (400 MHz, d_6-DMSO): δ 2.24 (s, 3H), 4.52 (s, 2H), 4.59 (s, 2H), 7.14 (s, 1H), 7.21 (t, $J = 7.8$ Hz, 1H), 7.30 (d, $J = 8$ Hz, 1H), 7.56 (m, 3H), 8.38 (dd, 1H), 8.46 (s, 1H), 8.96 (dd, 1H), 11.44 (s, 1H), 12.33 (s, 1H).

^{13}C NMR (125 MHz, d_6-DMSO): δ 20.0, 57.5, 68.7, 112.9, 116.6, 121.3, 122.0, 127.2, 127.5, 128.9, 129.2, 129.4, 130.1, 131.9, 135.4, 148.5, 150.2, 152.4, 152.8, 164.0.

HRMS (ESI, positive): calcd. for $C_{20}H_{19}N_3NaO_4$ $[M + Na]^+$ (m/z): 388.1273; found: 388.1275.

Synthesis of Zn^{2+} complex (BQ–Zn^{2+}) of receptor. The receptor, BQ (40 mg) and $ZnCl_2$ (10 mg) were mixed together and dissolved in 5 mL of methanol. After reflux for 12 hours the reaction mixture was cooled to room temperature. A reddish-yellow coloured precipitate appeared which was filtered and dried in vacuum.

HRMS (ESI, positive): calcd. for $C_{20}H_{18}ZnN_3NaO_4$ $[M + Zn^{2+} + Na^+ + H^+]^+$ (m/z): 451.0476; found: 451.0923.

Details of live-cell imaging

Materials methods. Frozen Human colorectal carcinoma cell lines HCT 116 (ATCC: CCL-247) were obtained from the American Type Culture Collection (Rockville, MD, USA) and maintained in Dulbecco's modified Eagle's medium (DMEM, Sigma Chemical Co., St. Louis, MO, USA) supplemented with 10% fetal bovine serum (Invitrogen), penicillin (100 μg mL^{-1}), and streptomycin (100 μg mL^{-1}). The RAW 264.7 macrophages were obtained from NCCS, Pune, India and maintained in DMEM containing 10% (v/v) fetal calf serum and antibiotics in a CO_2 incubator. Cells were initially propagated in 25 cm^2 tissue culture flask in an atmosphere of 5% CO_2 and 95% air at 37 °C humidified air till 70–80% confluency.

Fluorescent imaging studies. For fluorescent imaging studies, RAW cells, 7.5×10^3 cells in 150 μL media were seeded on sterile 12 mm diameter poly-l-lysine coated cover-slip and kept in a sterile 35 mm covered Petri dish and incubated at 37 °C in a CO_2 incubator for 24–30 h. Next day cells were washed three times with phosphate buffered saline (pH 7.4) and fixed using 4% paraformaldehyde in PBS (pH 7.4) for 10 minutes at room temperature washed with PBS followed by permeabilization using 0.1% saponin for 10 minutes. Then the cells were incubated with 2.0×10^{-5} M $ZnCl_2$ dissolved in 100 μL DMEM at 37 °C for 1 h in a CO_2 incubator and observed under 60× magnification of Andor spinning disc confocal

microscope. The cells were again washed thrice with PBS (pH 7.4) to remove any free metal and incubated in DMEM containing probe (BQ) to a final concentration of 1.0×10^{-5} M followed by washing with PBS (pH 7.4) three times to remove excess probe outside the cells. Again, images were acquired. Before fluorescent imaging all the solutions were aspirated out and cover slips containing cells were mounted on slides in a mounting medium containing DAPI, (4′,6-diamidino-2-phenylindole) in 1 μg mL^{-1} concentration. DAPI is a popular nuclear counterstain used in multicolor fluorescent imaging of cells. It preferentially stains dsDNA and its blue fluorescence stands out in contrast to green, yellow, or red fluorescent probes of other structures with little or no cytoplasmic labelling. Finally the slides were stored in dark before microscopic images are acquired.

Cytotoxicity assay. The cytotoxic effects of probe, $ZnCl_2$ and probe–$ZnCl_2$ complex were determined by an MTT assay following the manufacturer's instruction (MTT 2003, Sigma-Aldrich, MO). HCT cells were cultured into 96-well plates (approximately 10^4 cells per well) for 24 h. Next day media was removed and various concentrations of probe, $ZnCl_2$ and probe–$ZnCl_2$ complex (0, 15, 25, 50, 75, and 100 μM) made in DMEM were added to the cells and incubated for 24 h. Solvent control samples (cells treated with DMSO in DMEM), no cells and cells in DMEM without any treatment were also included in the study. Following incubation, the growth media were removed, and fresh DMEM containing MTT solution was added. The plate was incubated for 3–4 h at 37 °C. Subsequently, the supernatant was removed, the insoluble colored formazan product was solubilized in DMSO, and its absorbance was measured in a microtiter plate reader (Perkin-Elmer) at 570 nm. The assay was performed in triplicate for each concentration of probe, $ZnCl_2$ and probe–$CdCl_2$ complex. The OD value of wells containing only DMEM medium was subtracted from all readings to get rid of the background influence. Data analysis and calculation of standard deviation were performed with Microsoft Excel 2007 (Microsoft Corporation).

Conclusions

In summary, a new quinoline based probe BQ was synthesized, which is an excellent fluorescent sensor for detection of Zn^{2+}. This phenomenon was observed due to the ICT-CHEF mechanism only after introduction of Zn^{2+} in BQ solution. Zn^{2+} exhibits a tremendous increment in fluorescence intensity at 475 nm only after introduction of Zn^{2+} in BQ solution. The photophysical study shows that the probe forms 1 : 1 complex with Zn^{2+}. It produces a remarkably high selectivity toward Zn^{2+} ion over other competitive cations, such as Na^+, K^+, Mg^{2+}, Cu^{2+}, Mn^{2+}, Fe^{2+}, Fe^{3+}, Co^{2+}, Ni^{2+} and Hg^{2+}. The twist is in the fluorescence spectra with Cd^{2+} which shows fluorescence intensity at 465 nm. Most importantly, a discrimination of two metal ions (Zn^{2+} and Cd^{2+}) of almost similar characteristic can be achieved by the probe in hand. The detection limit was found to be in 10^{-8} M range. Moreover the probe BQ could be a suitable platform for Zn^{2+} imaging in biological system.

Acknowledgements

Authors thank the CSIR and DST, Govt. of India for financial supports. K.A and S.D acknowledge CSIR for providing them fellowships.

Notes and references

1 (*a*) P. N. Prasad, *Introduction to Biophotonics*, Wiley, NJ, 2003; (*b*) J. W. Lichtman and J.-A. Conchello, *Nat. Methods*, 2005, **2**, 910.

2 (*a*) J. M. Berg and Y. Shi, *Science*, 1996, **271**, 1081; (*b*) M. Lu and D. Fu, *Science*, 2007, **317**, 1746.

3 (*a*) C. J. Frederickson, J.-Y. Koh and A. I. Bush, *Nat. Rev. Neurosci.*, 2005, **6**, 449; (*b*) M. Cortesi, R. Chechik, A. Breskin, D. Vartsky, J. Ramon, G. Raviv, A. Volkov and E. Fridman, *Phys. Med. Biol.*, 2009, **54**, 781.

4 (*a*) E. Ho and B. N. Ames, *Proc. Natl. Acad. Sci. U. S. A.*, 2002, **99**, 16770; (*b*) H. Daiyasu, K. Osaka, Y. Ishino and H. Toh, *FEBS Lett.*, 2001, **503**, 1.

5 A. Q. Troung-Tran, J. Carter, R. E. Ruffin and P. D. Zalewski, *BioMetals*, 2001, **14**, 315.

6 (*a*) E. F. Rostan, H. V. DeBuys, D. L. Madey and S. R. Pinnell, *Int. J. Dermatol.*, 2002, **41**, 606; (*b*) Z. Szitányi, C. Nemes and N. Rozlosnik, *Central European Journal of Occupational and Environmental Medicine*, 1998, **4**, 51.

7 A. I. Bush, W. H. Pettingell, G. Multhaup, M. Paradis, J.-P. Vonsattel, J. F. Gusella, K. Beyreuther, C. L. Masters and R. E. Tanzi, *Science*, 1994, **265**, 1464.

8 (*a*) E. Tomat and S. J. Lippard, *Curr. Opin. Chem. Biol.*, 2010, **14**, 225; (*b*) Z. Xu, J. Yoon and D. R. Spring, *Chem. Soc. Rev.*, 2010, **39**, 1996; (*c*) E. L. Que, D. W. Domaille and C. J. Chang, *Chem. Rev.*, 2008, **108**, 1517; (*d*) P. Jiang and Z. Guo, *Coord. Chem. Rev.*, 2004, **248**, 205.

9 (*a*) A. P. de Silva, H. Q. N. Gunaratne, T. Gunnlaugsson, A. J. M. Huxley, C. P. McCoy, J. T. Rademacher and T. E. Rice, *Chem. Rev.*, 1997, **97**, 1515; (*b*) B. Valeur and I. Leray, *Coord. Chem. Rev.*, 2000, **205**, 3; (*c*) B. Valeur, *Molecular Fluorescence: Principles and Applications*, Wiley-VCH, Weinheim, 2001; (*d*) G. Sivaraman, T. Anand and D. Chellappa, *ChemPlusChem*, 2014, **79**, 1761; (*e*) T. Anand, G. Sivaraman, A. Mahesh and D. Chellappa, *Anal. Chim. Acta*, 2015, **853**, 596; (*f*) G. Sivaraman, B. Vidya and D. Chellappa, *RSC Adv.*, 2014, **4**, 30828; (*g*) L. E. Santos-Figueroa, M. E. Moragues, E. Climent, A. Agostini, R. Martínez-Máñez and F. Sancenón, *Chem. Soc. Rev.*, 2013, **42**, 3489; (*h*) S. Lee, K. K. Y. Yuen, K. A. Jolliffe and J. Yoon, *Chem. Soc. Rev.*, 2015, **44**, 1749; (*i*) N. A. Esipenko, P. Koutnik, T. Minami, L. Mosca, V. M. Lynch, G. V. Zyryanov and P. Anzenbacher Jr, *Chem. Sci.*, 2013, **4**, 3617; (*j*) S. Turkyilmaz, D. R. Rice, R. Palumbo and B. D. Smith, *Org. Biomol. Chem.*, 2014, **12**, 5645.

10 (*a*) K. R. Gee, Z. L. Zhou, W. J. Qian and R. Kennedy, *J. Am. Chem. Soc.*, 2002, **124**, 776; (*b*) E. J. Song, J. Kang, G. R. You, G. J. Park, Y. Kim, S.-J. Kim, C. Kim and R. G. Harrison, *Dalton Trans.*, 2013, **42**, 15514; (*c*) G. K. Tsikalas, P. Lazarou, E. Klontzas, S. A. Pergantis,

I. Spanopoulos, P. N. Trikalitis, G. E. Froudakis and H. E. Katerinopoulos, *RSC Adv.*, 2014, **4**, 693; (*d*) K. B. Kim, H. Kim, E. J. Song, S. Kim, I. Noh and C. Kim, *Dalton Trans.*, 2013, **42**, 16569; (*e*) P. Li, X. Zhou, R. Huang, L. Yang, X. Tang, W. Dou, Q. Zhao and W. Liu, *Dalton Trans.*, 2014, **43**, 706; (*f*) Z. Liu, C. Zhang, Y. Chen, F. Qian, Y. Bai, W. He and Z. Guo, *Chem. Commun.*, 2014, **50**, 1253; (*g*) T.-T. Zhang, X.-P. Chen, J.-T. Liu, L.-Z. Zhang, J.-M. Chu, L. Su and B.-X. Zhao, *RSC Adv.*, 2014, **4**, 16973; (*h*) V. Bhalla, Roopa and M. Kumar, *Dalton Trans.*, 2013, **42**, 975; (*i*) Z. Xu, K.-H. Baek, H. N. Kim, J. Cui, X. Qian, D. R. Spring, I. Shin and J. Yoon, *J. Am. Chem. Soc.*, 2010, **132**, 601; (*j*) N. Y. Baek, C. H. Heo, C. S. Lim, G. Masanta, B. R. Cho and H. M. Kim, *Chem. Commun.*, 2012, **48**, 4546; (*k*) B. K. Datta, D. Thiyagarajan, S. Samanta, A. Ramesh and G. Das, *Org. Biomol. Chem.*, 2014, **12**, 4975; (*l*) J. Pancholi, D. J. Hodson, K. Jobe, G. A. Rutter, S. M. Goldup and M. Watkinson, *Chem. Sci.*, 2014, **5**, 3528; (*m*) Z. Dong, X. Le, P. Zhou, C. Dong and J. Ma, *New J. Chem.*, 2014, **38**, 1802; (*n*) P. Li, X. Zhou, R. Huang, L. Yang, X. Tang, W. Dou, Q. Zhao and W. Liu, *Dalton Trans.*, 2014, **43**, 706; (*o*) Y. Xu, L. Xiao, S. Sun, Z. Pei, Y. Pei and Y. Pang, *Chem. Commun.*, 2014, **50**, 7514; (*p*) N. Khairnar, K. Tayade, S. K. Sahoo, B. Bondhopadhyay, A. Basu, J. Singh, N. Singh, V. Gite and A. Kuwar, *Dalton Trans.*, 2015, **44**, 2097; (*q*) G. Sivaraman, T. Anand and D. Chellappa, *Analyst*, 2012, **137**, 5881; (*r*) P. Kaleeswaran, I. A. Azath, V. Tharmaraj and K. Pitchumani, *ChemPlusChem*, 2014, **79**, 1361; (*s*) G. Sivaraman, T. Anand and D. Chellappa, *Anal. Methods*, 2014, **6**, 2343; (*t*) E. M. Nolan and S. J. Lippard, *Acc. Chem. Res.*, 2009, **42**, 193; (*u*) H. T. Ngo, X. Liu and K. A. Jolliffe, *Chem. Soc. Rev.*, 2012, **41**, 4928.

11 (*a*) S. Goswami, S. Das, K. Aich, D. Sarkar and T. K. Mondal, *Tetrahedron Lett.*, 2013, **54**, 6892; (*b*) S. Goswami, S. Das, K. Aich, D. Sarkar and T. K. Mondal, *Tetrahedron Lett.*, 2014, **55**, 2695; (*c*) S. Goswami, K. Aich, S. Das, S. B. Roy, B. Pakhira and S. Sarkar, *RSC Adv.*, 2014, **4**, 14210; (*d*) S. Goswami, K. Aich, S. Das, A. K. Das, A. Manna and S. Halder, *Analyst*, 2013, **138**, 1903; (*e*) S. Goswami, K. Aich and D. Sen, *Chem. Lett.*, 2012, **41**, 863; (*f*) S. Goswami, S. Das, K. Aich, D. Sarkar, T. K. Mondal, C. K. Quah and H.-K. Fun, *Dalton Trans.*, 2013, **42**, 15113; (*g*) S. Goswami, S. Das, K. Aich, B. Pakhira, S. Panja, S. K. Mukherjee and S. Sarkar, *Org. Lett.*, 2013, **15**, 5412; (*h*) S. Goswami, S. Das and K. Aich, *Tetrahedron Lett.*, 2013, **54**, 4620; (*i*) S. Goswami, K. Aich, S. Das, A. K. Das, D. Sarkar, S. Panja, T. K. Mondal and S. K. Mukhopadhyay, *Chem. Commun.*, 2013, **49**, 10739; (*j*) S. Goswami, K. Aich, S. Das, B. Pakhira, K. Ghoshal, C. K. Quah, M. Bhattacharyya, H.-K. Fun and S. Sarkar, *Chem.–Asian J.*, 2015, **10**, 694; (*k*) S. Goswami, K. Aich, S. Das, C. D. Mukhopadhyay, D. Sarkar and T. K. Mondal, *Dalton Trans.*, 2015, **44**, 5763.

12 S. Goswami, K. Aich, A. K. Das, A. Manna and S. Das, *RSC Adv.*, 2013, **3**, 2412.

13 (*a*) H. A. Benesi and J. H. Hildebrand, *J. Am. Chem. Soc.*, 1949, **71**, 2703; (*b*) D. C. Carter and J. X. Ho, *Adv. Protein Chem.*, 1994, **45**, 153; (*c*) A. Mallick and N. Chattopadhyay, *Photochem. Photobiol.*, 2005, **81**, 419; (*d*) I. Ravikumar, B. N. Ahamed and P. Ghosh, *Tetrahedron*, 2007, **63**, 12940.

14 (*a*) M. Shortreed, R. Kopelman, M. Kuhn and B. Hoyland, *Anal. Chem.*, 1996, **68**, 1414; (*b*) W. Lin, L. Yuan, Z. Cao, Y. Feng and L. Long, *Chem.–Eur. J.*, 2009, **15**, 5096.

